A Letters Journal Exploring the Frontiers of Physics

May 2014

EPL, **106** (2014) 39001
doi: 10.1209/0295-5075/106/39001

www.epljournal.org

Subexponential decay in Fermi-LAT pulsar spectra: The case for tachyonic Cherenkov radiation

Roman Tomaschitz[a]

Department of Physics, Hiroshima University - 1-3-1 Kagami-yama, Higashi-Hiroshima 739-8526, Japan

received 3 February 2014; accepted in final form 22 April 2014
published online 15 May 2014

PACS 95.30.Gv – Radiation mechanisms; polarization
PACS 41.60.Bq – Cherenkov radiation
PACS 97.60.Gb – Pulsars

Abstract – Tachyonic Cherenkov fits are performed to the Fermi-LAT γ-ray spectra of the Vela pulsar, PSR J1709 − 4429 and Geminga. The high-energy spectral tails of these pulsars exhibit pronounced subexponential Weibull decay, which can be modeled in a permeable spacetime by a frequency-dependent tachyon mass. The scaling exponent of the tachyon mass defines the Weibull shape parameter of the energy flux, and it also determines whether the radiation is sub- or superluminal. The negative mass-square in the tachyonic Maxwell-Proca equations gives rise to a longitudinal flux component. The radiation is generated by an ultra-relativistic thermal electron plasma via the inertial Cherenkov effect. The transversal and longitudinal γ-ray emission from Geminga is slightly superluminal, whereas γ-rays from the Vela pulsar and PSR J1709 − 4429 are subluminal despite the negative tachyonic mass-square in the dispersion relations.

Introduction. – In the 2nd Fermi-LAT pulsar catalog [1], the energy flux of several pulsars shows weaker-than-exponential decay in the low GeV band, for instance, the Vela pulsar (PSR J0835 − 4510) [2] and PSR J1709 − 4429 [3], as well as the Crab pulsar (PSR J0534+2200) [4], PSR J1836 + 5925 [5], Geminga (PSR J0633 + 1746) [6], and PSR J2021 + 4026 [7]. The subexponential decay of the γ-ray spectral tails can be explained by tachyonic Cherenkov emission from a thermal electron plasma.

First, we briefly outline the radiation mechanism, the coupling of tachyonic radiation fields to a dispersive permeability tensor, the Maxwell-Proca equations with negative mass-square, the Lagrangian and the dispersion relations, all in space-frequency representation suitable for frequency-dependent permeabilities, cf. (1)–(7). We discuss the tachyonic Cherenkov densities generated by a uniformly moving subluminal charge in a dispersive spacetime and explain the frequency scaling of the tachyon mass and the tachyonic fine-structure constant, cf. (8)–(13). We average the spectral densities with relativistic electron distributions and derive the transversal and longitudinal polarization components of the tachyonic energy flux, cf. (14)–(25). We study the high- and intermediate-energy regimes, in particular the Weibull decay $\propto \exp(-\beta_\infty E^{1-\rho})$ of the spectral tail, where ρ is the scaling exponent of the tachyon mass, $m_{\rm t}(E) = m_{\rm t0}E^\rho$, and β_∞ is a decay constant related to the electron temperature and the tachyonic mass amplitude $m_{\rm t0}$, cf. (26)–(30). We perform spectral fits to the Fermi-LAT spectra of the Vela pulsar, PSR J1709 − 4429 and Geminga, extracting the scaling exponents of the tachyon mass and the tachyonic fine-structure constant, cf. figs. 1–3, and explain how sub- and superluminal group velocities in the γ-ray band are related to the Weibull shape parameter, cf. (31).

Maxwell-Proca fields with negative mass-square. – We summarize the basic equations to keep the paper self-contained; details can be found in [8,9]. The Fourier time-transform of the tachyonic vector potential $A_\mu = (A_0, \mathbf{A})$ is defined by $\hat{A}_\mu(\mathbf{x},\omega) = \int_{-\infty}^{\infty} A_\mu(\mathbf{x},t)\mathrm{e}^{\mathrm{i}\omega t}\mathrm{d}t$, and the same convention applies for field strengths, inductions and currents. The homogeneous Maxwell equations read $\mathrm{rot}\hat{\mathbf{E}} - \mathrm{i}\omega\hat{\mathbf{B}} = 0$, $\mathrm{div}\hat{\mathbf{B}} = 0$. The field strengths $\hat{\mathbf{E}}(\mathbf{x},\omega)$ and $\hat{\mathbf{B}}(\mathbf{x},\omega)$ are related to the vector potential by $\hat{\mathbf{E}} = \mathrm{i}\omega\hat{\mathbf{A}} + \nabla\hat{A}_0$, $\hat{\mathbf{B}} = \mathrm{rot}\hat{\mathbf{A}}$. The constitutive relations defining the inductions $\hat{\mathbf{D}}$ and $\hat{\mathbf{H}}$ and the inductive potential $\hat{C}_\mu = (\hat{C}_0, \hat{\mathbf{C}})$ are

$$\hat{\mathbf{D}}(\mathbf{x},\omega) = \varepsilon(\omega)\hat{\mathbf{E}}(\mathbf{x},\omega), \qquad \hat{\mathbf{B}}(\mathbf{x},\omega) = \mu(\omega)\hat{\mathbf{H}}(\mathbf{x},\omega),$$
$$\hat{\mathbf{A}}(\mathbf{x},\omega) = \mu_0(\omega)\hat{\mathbf{C}}(\mathbf{x},\omega), \quad \hat{C}_0(\mathbf{x},\omega) = \varepsilon_0(\omega)\hat{A}_0(\mathbf{x},\omega). \quad (1)$$

[a]E-mail: tom@geminga.org

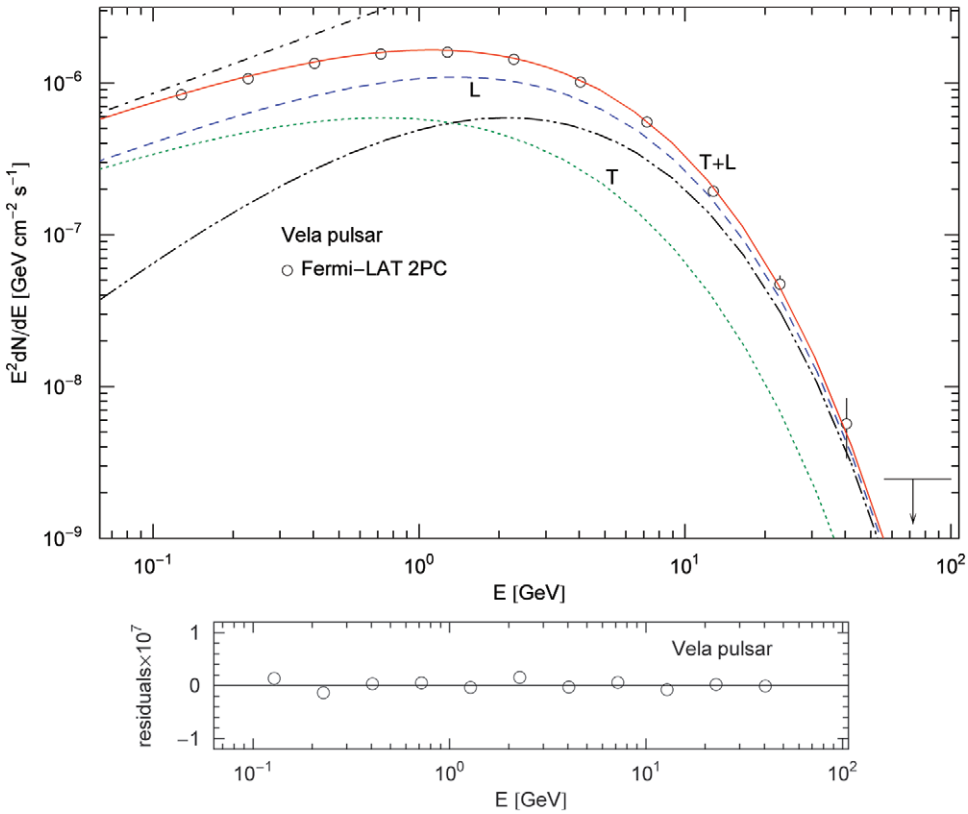

Fig. 1: (Colour on-line) Tachyonic γ-ray spectrum of the Vela pulsar. Data points from Fermi-LAT (Large Area Telescope, 2nd Pulsar Catalog) [1]. The solid curve T + L depicts the unpolarized tachyonic energy flux $EF_E^{\mathrm{T+L}} = E^2\mathrm{d}N^{\mathrm{T+L}}/\mathrm{d}E$, cf. (22) and (25), obtained by adding the transversal flux component EF_E^{T} (dotted curve, labeled T) and the longitudinal component EF_E^{L} (dashed curve, L). The polarization components $EF_E^{\mathrm{T,L}}$ are compiled in (20)–(22). The dot-dashed and double-dot–dashed curves depict the asymptotic limits of $EF_E^{\mathrm{T+L}}$; the power-law ascent (28) is followed by a cross-over into subexponential Weibull decay, cf. (26) and table 1. (7 dof, $\chi^2 \approx 21$.)

The permeabilities ε, μ, μ_0 and ε_0 are positive and dimensionless. As the inductions are real, the permeabilities satisfy $\varepsilon(\omega) = \varepsilon(-\omega)$, etc. In vacuum, $\varepsilon = \varepsilon_0 = 1$ and $\mu = \mu_0 = 1$ (Heaviside-Lorentz system). The inhomogeneous field equations coupled to a current $\hat{j}^\mu_\Omega = (\hat{\rho}_\Omega, \hat{\mathbf{j}}_\Omega)$, cf. after (5), read

$$\mathrm{rot}\hat{\mathbf{H}} + \mathrm{i}\omega\hat{\mathbf{D}} = \hat{\mathbf{j}}_\Omega + m_\mathrm{t}^2(\omega)\hat{\mathbf{C}}, \quad \mathrm{div}\hat{\mathbf{D}} = \hat{\rho}_\Omega - m_\mathrm{t}^2(\omega)\hat{C}_0. \quad (2)$$

We take the divergence of the first equation, substitute the second and use current conservation $\mathrm{i}\omega\hat{\rho}_\Omega - \mathrm{div}\hat{\mathbf{j}}_\Omega = 0$ to obtain the Lorentz condition $\mathrm{div}\hat{\mathbf{C}} + \mathrm{i}\omega\hat{C}_0 = 0$, due to the tachyonic mass-square $m_\mathrm{t}^2(\omega)$. ($m_\mathrm{t}^2 > 0$ with the sign convention in (2) and (3).) The energy flux vector is $\hat{\mathbf{S}} = \hat{\mathbf{E}} \times \hat{\mathbf{H}}^* + m_\mathrm{t}^2 \hat{A}_0 \hat{\mathbf{C}}^* + \mathrm{c.c.}$ The field equations can be derived from the Lagrangian

$$\hat{L} = -\frac{1}{4}\hat{F}_{\mu\nu} g_F^{\mu\alpha} g_F^{\nu\beta} \hat{F}^*_{\alpha\beta} + \frac{1}{2} m_\mathrm{t}^2 \hat{A}_\mu g_A^{\mu\nu} \hat{A}^*_\nu + \frac{1}{2}(\hat{A}_\mu g_J^{\mu\nu} \hat{j}^*_\nu + \hat{A}^*_\mu g_J^{\mu\nu} \hat{j}_\nu), \quad (3)$$

where $\hat{F}_{\mu\nu}(\mathbf{x}, \omega)$ is the Fourier transform of the field tensor $F_{\mu\nu}(\mathbf{x}, t) = A_{\nu,\mu} - A_{\mu,\nu}$. The tachyonic radiation field is modeled after electrodynamics, a Proca field with negative mass-square, minimally coupled to an electron current in a dispersive spacetime, the Minkowski metric being replaced by permeability tensors $g^{\mu\nu}_{F,A,J}(\omega)$. A space-frequency representation is employed to avoid clumsy time convolutions of the inductive fields. The first term in (3) containing $g_F^{\mu\nu}$ is analogous to the electrodynamic Lagrangian in a dielectric medium, in manifestly covariant notation. A second permeability tensor $g_A^{\mu\nu}$ enters in the mass term, resulting in different dispersion relations and group velocities for transversal and longitudinal modes, cf. (4) and (7). The meaning of permeability tensor $g_J^{\mu\nu}$ in the interaction term is explained after (5).

A distinct difference of tachyonic Cherenkov radiation as compared to electromagnetic radiation, Cherenkov, synchrotron or otherwise, is the potential sub- or super-exponential decay of γ-ray spectral tails, once the spectral densities are averaged over a thermal or non-thermal electron distribution. In contrast, electromagnetic radiation mechanisms lead to strictly linear exponential decay of the averaged spectral densities. The subexponential Weibull decay $\propto \exp(-\beta_\infty E^{1-\rho})$ (see the introduction) observed in the spectral tails of the mentioned pulsars is pronounced, the power-law exponents ρ listed in table 1 substantially differ from zero. It would not be possible

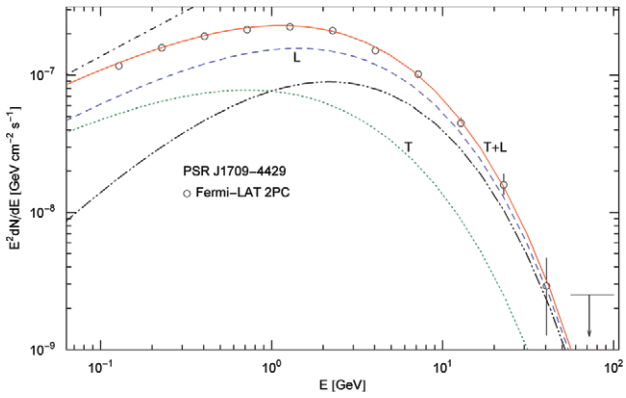

Fig. 2: (Colour on-line) Tachyonic energy flux of pulsar PSR J1709 − 4429. Data points from Fermi-LAT [1]. Description of the curves as in fig. 1; the fitting parameters are listed in table 1. The transversal radiation is linearly polarized and weaker than the longitudinal component. The spectral shape and parameters are similar to the Vela spectrum in fig. 1, apart from the lower flux amplitude partially due to the increased distance $d \approx 2.3\,\mathrm{kpc}$ ($d \approx 0.29\,\mathrm{kpc}$ for the Vela pulsar). (7 dof, $\chi^2 \approx 11$.)

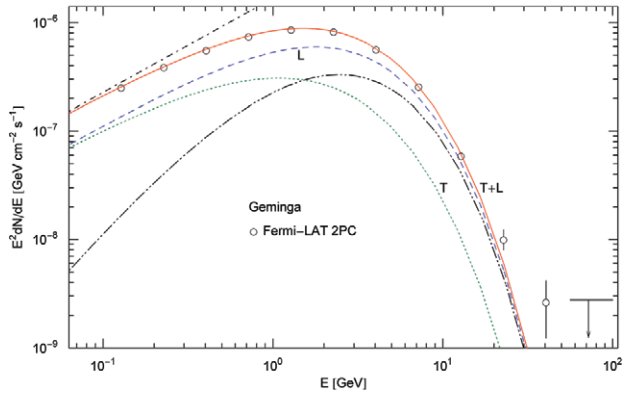

Fig. 3: (Colour on-line) Tachyonic spectral map of Geminga. Data points from Fermi-LAT [1]. Description of the curves as in fig. 1. The ascending slope is steeper than in figs. 1 and 2, since the fine-structure scaling exponent σ is close to zero, cf. table 1. The mass scaling exponent ρ lies below 1/2, which results in a rapid spectral cutoff, cf. (26), and renders the radiation superluminal, cf. (31). The distance estimate is 0.25 kpc. (7 dof, $\chi^2 \approx 11$.)

to fit the γ-ray spectra in figs. 1–3 with a logarithmic correction to a linear exponential. The conceptually most important difference to electromagnetic radiation is superluminality, which arises for $\rho < 1/2$ due to the tachyonic mass-square. If the decay is weak, $\rho \geq 1/2$, the velocity of the radiated quanta is subluminal despite the mass term in (3). Here, we show how the shape parameter $1 - \rho$ of tachyonic Cherenkov spectra can be used to distinguish subluminal from superluminal group velocities of γ-rays close to the speed of light.

Another marked difference to electromagnetic spectra owing to the tachyonic mass-square in Lagrangian (3) is longitudinal polarization. Especially in the classical

Table 1: Fitting parameters of the tachyonic energy flux of the pulsars in figs. 1–3. Recorded are the fine-structure scaling exponent σ and the scaling exponent ρ of the tachyon mass, cf. (10) and (26), the decay exponent $\beta_\infty = \sqrt{\varepsilon\mu_0}\beta/m_{\mathrm{t}0}[\mathrm{GeV}]$, cf. (17) and (27), and the flux amplitude a_t [GeV cm^{-2}s^{-1}], cf. (24). The spectral fits are based on the differential flux density $EF_E^{\mathrm{T+L}} = E^2\mathrm{d}N^{\mathrm{T+L}}/\mathrm{d}E$, cf. (25). The γ-rays are radiated by a thermal ultra-relativistic plasma with electron index $\alpha = -2$.

	σ	ρ	β_∞	a_t
Vela	−0.443	0.543	2.404	5.43×10^{-6}
J1709	−0.558	0.611	2.743	1.19×10^{-6}
Geminga	−0.0186	0.444	2.159	1.96×10^{-6}

Cherenkov regime, where the tachyon-electron mass ratio is small, $m_\mathrm{t}(\omega)/m_\mathrm{e} \ll 1$, there is a substantial longitudinal radiation component, see figs. 1–3, and the weaker transversal radiation is linearly polarized, that is, there is only one degree of transversal polarization. If one just uses Stokes parameters to analyze the polarization, one will mistakenly identify the longitudinal component as transversal, as these parameters are based on the assumption of transversality. In the extreme quantum regime, where $m_\mathrm{t}(\omega)/m_\mathrm{e} \gg 1$ (which can be reached in TeV spectra because of the frequency dependence of the tachyon mass), there emerge two transversal degrees of comparable magnitude as well as a weaker longitudinal radiation component, but this is not the case for the pulsar spectra discussed here.

The 3D field strengths are $\hat{E}_k = \hat{F}_{k0}$ and $\hat{B}^k = \varepsilon^{kij}\hat{F}_{ij}/2$. The Fourier transform of the 4-current $j^\mu = (\rho, \mathbf{j})$ is denoted by $\hat{j}^\mu = (\hat{\rho}, \hat{\mathbf{j}})$ in Lagrangian (3). The permeabilities in (1) define isotropic tensors $g_A^{\mu\nu}(\omega)$ and $g_F^{\mu\nu}(\omega)$,

$$g_A^{00} = -\varepsilon_0, \quad g_A^{ij} = \frac{\delta^{ij}}{\mu_0}, \quad g_F^{00} = -\mu^{1/2}\varepsilon, \quad g_F^{ij} = \frac{\delta^{ij}}{\mu^{1/2}}, \tag{4}$$

with $g_A^{0i} = g_F^{0i} = 0$. The permeability tensor $g_J^{\mu\nu}(\omega)$ couples the external current to the field,

$$g_J^{00} = -\Omega_0(\omega), \qquad g_J^{mn} = \frac{\delta^{mn}}{\Omega(\omega)}, \qquad g_J^{k0} = 0. \tag{5}$$

Greek indices are raised and lowered with the Minkowski metric $\eta_{\mu\nu} = \mathrm{diag}(-1, 1, 1, 1)$. The inductive 4-potential is $\hat{C}_\mu = (\hat{C}_0, \hat{\mathbf{C}})$ or $\hat{C}^\mu = g_A^{\mu\nu}\hat{A}_\nu$, and the inductive field tensor reads $\hat{H}^{\mu\nu} = g_F^{\mu\alpha}g_F^{\nu\beta}\hat{F}_{\alpha\beta}$. The inductions in (1) are related to $\hat{H}^{\mu\nu}$ by $\hat{D}^l = \hat{H}^{0l}$ and $\hat{H}_i = \varepsilon_{ikl}\hat{H}^{kl}/2$.

The "dressed" current $\hat{j}_\Omega^\mu = (\hat{\rho}_\Omega, \hat{\mathbf{j}}_\Omega)$ in the field equations (2) is defined by $\hat{j}_\Omega^\mu = g_J^{\mu\nu}\hat{j}_\nu$, cf. (3). The tensor $g_J^{\mu\nu}$ amounts to a varying coupling constant if $\Omega_0(\omega)$ coincides with $1/\Omega(\omega)$ [9], which is assumed in the following, cf. (10) and table 1. Thus, $\hat{j}_\Omega^\mu = \hat{j}^\mu/\Omega(\omega)$ or $\hat{j}_\Omega^\mu = (\hat{\rho}/\Omega, \hat{\mathbf{j}}/\Omega)$. If the external current is conserved, $\hat{j}^m_{,m} - \mathrm{i}\omega\hat{j}^0 = 0$, this holds true for $\hat{j}_\Omega^\mu$ as well, so that the field equations for

the vector potential read

$$(\Delta + k_{\rm L}^2(\omega))\hat{A}_0 = \frac{1}{\varepsilon}\hat{\rho}_\Omega,$$
$$(\Delta + k_{\rm T}^2(\omega))\hat{\mathbf{A}} + \left(\frac{\varepsilon}{\varepsilon_0}\frac{\mu}{\mu_0} - 1\right)\nabla{\rm div}\hat{\mathbf{A}} = -\mu\hat{\mathbf{j}}_\Omega, \tag{6}$$

$$k_{\rm T}^2(\omega) = \varepsilon\mu\omega^2 + m_{\rm t}^2\frac{\mu}{\mu_0}, \qquad k_{\rm L}^2(\omega) = \varepsilon_0\mu_0\omega^2 + m_{\rm t}^2\frac{\varepsilon_0}{\varepsilon}. \tag{7}$$

The Proca equations (6) and dispersion relations (7) are equivalent to the Maxwell equations (2) with conserved current. Transversal waves satisfy ${\rm div}\hat{\mathbf{A}} = 0$, longitudinal ones ${\rm rot}\hat{\mathbf{A}} = 0$.

Tachyonic Cherenkov densities of an inertial charge in a permeable spacetime. – We consider a classical charge q moving with constant subluminal velocity $\upsilon < 1$. The charge and current densities are $\rho = q\delta(\mathbf{x} - \boldsymbol{\upsilon}t)$ and $\mathbf{j}(\mathbf{x}, t) = q\boldsymbol{\upsilon}\delta(\mathbf{x} - \boldsymbol{\upsilon}t)$. In [9], we calculated the tachyonic radiation fields of this current via the Proca equations (6) and (7), and derived the asymptotic Poynting vectors and the power $P^{\rm T,L}$ transversally and longitudinally radiated:

$$P^{\rm T} = \int_0^{\omega_{\rm T,max}} p^{\rm T}(\omega){\rm d}\omega, \qquad P^{\rm L} = \int_0^{\omega_{\rm L,max}} p^{\rm L}(\omega){\rm d}\omega, \tag{8}$$

$$p^{\rm T}(\omega) = \frac{q^2}{4\pi\Omega^2(\omega)}\left(1 - \frac{\omega^2}{k_{\rm T}^2(\omega)\upsilon^2}\right)\mu(\omega)\omega\upsilon,$$
$$p^{\rm L}(\omega) = \frac{q^2}{4\pi\Omega^2(\omega)}\frac{m_{\rm t}^2(\omega)\varepsilon_0(\omega)\omega}{\varepsilon^2(\omega)k_{\rm L}^2(\omega)\upsilon}. \tag{9}$$

The integration of the classical densities in (8) is over frequency intervals in which $k_{\rm T}(\omega)\upsilon > \omega$ and $k_{\rm L}(\omega)\upsilon > \omega$ respectively, cf. (7). Here, we assume that equation $k_{\rm T}(\omega_{\rm T,max})\upsilon = \omega_{\rm T,max}$ has just one solution and $k_{\rm T}(\omega)\upsilon > \omega$ for $\omega < \omega_{\rm T,max}$, and analogously for the longitudinal power $P^{\rm L}$ and $\omega_{\rm L,max}$. We will consider constant positive permeabilities with $\varepsilon\mu = 1$ and $\varepsilon_0\mu_0 = 1$, so that the transversal and longitudinal dispersion relations (7) coincide. Radiation from uniformly moving subluminal charges is generated by the Cherenkov mechanism [10,11]. The radiated tachyonic quanta can be sub- or superluminal, cf. (31). Apart from the inertial Cherenkov effect, electromagnetic radiation by transversal and longitudinal acceleration of superluminal charges has been studied in [12], and radiation from superluminally rotating macroscopic light spots in [13]. As the electron plasma is magnetically confined, there is also tachyonic synchrotron radiation inducing ripples in the radiation densities (9) [14]. Averaged over the electron density (14), this radiation is negligible compared with the inertial emission caused by the negative mass-square [15].

We measure energy in GeV units, writing E for $\hbar\omega[\,{\rm GeV}]$, and consider a power-law frequency variation of the tachyon mass and the tachyonic fine-structure constant,

$$m_{\rm t}(E) = m_{\rm t0}E^\rho, \qquad \alpha_{\rm t}(E) = \frac{q^2}{4\pi\Omega^2} = \alpha_{\rm t0}E^\sigma. \tag{10}$$

Here, we have identified the scaling function $\Omega(\omega)$ in (5) and (9) as $\Omega = E^{-\sigma/2}$. The amplitude $\alpha_{\rm t0} = q^2/(4\pi\hbar c)$ is dimensionless, being the tachyonic counterpart to the electric fine-structure constant $e^2/(4\pi\hbar c) = 1/137$. $\alpha_{\rm t0}$ and $m_{\rm t0}[\,{\rm GeV}]$ are positive amplitudes. The mass scaling exponent ρ is restricted to $\rho < 1$, see after (21). In the range $0 < \rho < 1$, we will find subexponential decay $\propto \exp(-\beta_\infty E^{1-\rho})$ of the energy flux, cf. (26).

We substitute the wave numbers (7) into the spectral densities (9) and parametrize the velocity of the subluminal charge with the Lorentz factor, $\upsilon = \sqrt{\gamma^2 - 1}/\gamma$,

$$p^{\rm T}(E,\gamma) = \frac{q^2}{4\pi\Omega^2\varepsilon}\frac{m_{\rm t}^2 E}{\varepsilon\mu_0 E^2 + m_{\rm t}^2}\left(1 - \frac{1}{\eta(\gamma)}\frac{E^2}{m_{\rm t}^2}\right)\frac{\sqrt{\gamma^2-1}}{\gamma},$$
$$p^{\rm L}(E,\gamma) = \frac{q^2}{4\pi\Omega^2\varepsilon}\frac{m_{\rm t}^2 E}{\varepsilon\mu_0 E^2 + m_{\rm t}^2}\frac{\gamma}{\sqrt{\gamma^2-1}}, \tag{11}$$

where we use the shortcut

$$\eta(\gamma) = \frac{1}{\varepsilon\mu_0}(\gamma^2 - 1). \tag{12}$$

Equation $E_{\rm max}^2 = m_{\rm t}^2(E_{\rm max})\eta(\gamma)$ is equivalent to $k_{\rm T,L}(\omega_{\rm max})\upsilon = \omega_{\rm max}$, as the dispersion relations (7) are identical for $\varepsilon_0\mu_0 = \varepsilon\mu$, cf. after (9), so that $\omega_{\rm T,max} = \omega_{\rm L,max}$ in (8) and $E_{\rm max} = \hbar\omega_{\rm max}[\,{\rm GeV}]$. Substituting $m_{\rm t}(E) = m_{\rm t0}E^\rho$, cf. (10), we can solve for $E_{\rm max}$ to find the highest frequency radiated by an inertial charge with Lorentz factor γ,

$$E_{\rm max}(\gamma) = m_{\rm t0}^{1/(1-\rho)}(\eta(\gamma))^{1/(2-2\rho)}. \tag{13}$$

Since $\rho < 1$, $E_{\rm max}(\gamma)$ is monotonically increasing. For the classical densities (9) to be applicable, $E_{\rm max}(\gamma) \ll m_{\rm e}\gamma$ has to hold, where $m_{\rm e}\gamma$ is the energy of the radiating charge.

Polarized radiation densities averaged over thermal and non-thermal electron distributions. – We average the radiation densities (11) over an electronic power-law distribution [16],

$${\rm d}\rho_{\alpha,\beta}(\gamma) = A_{\alpha,\beta}\gamma^{-\alpha-1}{\rm e}^{-\beta\gamma}\sqrt{\gamma^2-1}{\rm d}\gamma, \tag{14}$$

parametrized with the electronic Lorentz factor γ. The dimensionless normalization constant $A_{\alpha,\beta}$ is related to the electron number $N_{\rm e} = A_{\alpha,\beta}K_{\alpha,\beta}$ by

$$K_{\alpha,\beta} = \int_1^\infty \gamma^{-\alpha-1}{\rm e}^{-\beta\gamma}\sqrt{\gamma^2-1}{\rm d}\gamma, \tag{15}$$

where $\beta = m_{\rm e}/(k_{\rm B}T)$ is the dimensionless temperature parameter and $m_{\rm e}$ the electron mass, so that $T[\,{\rm K}] \approx 5.93 \times 10^9/\beta$. A Maxwell-Boltzmann equilibrium distribution requires the electron index $\alpha = -2$; $K_{\alpha=-2,\beta} = K_2(\beta)/\beta$ is a modified Bessel function.

The spectral average of the radiation densities (11) is carried out as

$$\langle p^{\mathrm{T,L}}(E)\rangle_{\alpha,\beta} = \int_1^\infty p^{\mathrm{T,L}}(E,\gamma)\theta(E_{\max}(\gamma)-E)\mathrm{d}\rho_{\alpha,\beta}(\gamma), \tag{16}$$

where θ is the Heaviside step function. We solve the inequality $E < E_{\max}(\gamma)$ for γ, with $E_{\max}(\gamma)$ in (13): $\gamma > \gamma_{\min}(E)$,

$$\gamma_{\min}(E) = \sqrt{1+\kappa_{\mathrm{t}}^2 E^{2(1-\rho)}}, \quad \kappa_{\mathrm{t}} = \frac{\sqrt{\varepsilon\mu_0}}{m_{\mathrm{t}0}[\mathrm{GeV}]}. \tag{17}$$

$\gamma_{\min}(E)$ is monotonically increasing for $\rho < 1$. For a frequency E to be radiated, this requires the Lorentz factor to exceed $\gamma_{\min}(E)$. The average (16) can thus be reduced to

$$\langle p^{\mathrm{T,L}}(E)\rangle_{\alpha,\beta} = B^{\mathrm{T,L}}(E,\gamma_{\min}(E)), \tag{18}$$

$$B^{\mathrm{T,L}}(E,\gamma_{\min}) = \int_{\gamma_{\min}}^\infty p^{\mathrm{T,L}}(E,\gamma)\mathrm{d}\rho_{\alpha,\beta}(\gamma). \tag{19}$$

More explicitly, the transversal/longitudinal spectral functions $B^{\mathrm{T,L}}$ read

$$\begin{aligned} B^{\mathrm{T}}(E,\gamma_{\min}) &= A_{\alpha,\beta}\frac{1}{\varepsilon}\frac{\alpha_{\mathrm{t}}(E)E}{\beta^2\gamma_{\min}^{\alpha+3}}\Big[(\alpha(\alpha+1)-(\beta\gamma_{\min})^2) \\ &\quad\times(\beta\gamma_{\min})^{\alpha+1}\Gamma(-\alpha-1,\beta\gamma_{\min}) \\ &\quad+\mathrm{e}^{-\beta\gamma_{\min}}(\beta\gamma_{\min}-\alpha)\Big], \end{aligned} \tag{20}$$

$$\begin{aligned} B^{\mathrm{L}}(E,\gamma_{\min}) &= A_{\alpha,\beta}\frac{1}{\varepsilon}\frac{\alpha_{\mathrm{t}}(E)E}{\beta^2\gamma_{\min}^{\alpha+3}}\Big[\alpha(\alpha+1)(\beta\gamma_{\min})^{\alpha+1} \\ &\quad\times\Gamma(-\alpha-1,\beta\gamma_{\min})+\mathrm{e}^{-\beta\gamma_{\min}}(\beta\gamma_{\min}-\alpha)\Big]. \end{aligned} \tag{21}$$

We write $B^{\mathrm{T,L}}(E)$ for $B^{\mathrm{T,L}}(E,\gamma_{\min}(E))$. The unpolarized radiation density is $\langle p^{\mathrm{T+L}}(E)\rangle_{\alpha,\beta} = B^{\mathrm{T+L}}(E)$, with $B^{\mathrm{T+L}} = B^{\mathrm{T}} + B^{\mathrm{L}}$. For a thermal electron distribution, $\alpha = -2$, the spectral functions simplify since $\Gamma(1,\beta\gamma_{\min}) = \mathrm{e}^{-\beta\gamma_{\min}}$. The asymptotic limit of the incomplete gamma function is $\Gamma(-\alpha-1,\beta\gamma_{\min}) \sim (\beta\gamma_{\min})^{-\alpha-2}\mathrm{e}^{-\beta\gamma_{\min}}$, applicable for $\beta\gamma_{\min}(E) \gg 1$, so that the spectral functions $B^{\mathrm{T,L}}(E)$ decay subexponentially ($0 < \rho < 1$) or superexponentially ($\rho < 0$) for $E \to \infty$, cf. (17). The minimal Lorentz factor $\gamma_{\min}(E)$ in (17) remains valid for $\rho \geq 1$, but the limit $\gamma_{\min}(E\to\infty)$ is finite, so that a genuine exponential decay factor is lacking in the spectral functions. Therefore we restrict the mass scaling exponent to $\rho < 1$.

The differential energy flux $F_E^{\mathrm{T,L}}$ and the differential number flux $\mathrm{d}N^{\mathrm{T,L}}/\mathrm{d}E$ are related to the spectral functions $B^{\mathrm{T,L}}(E)$ by, cf. (18),

$$E^k F_E^{\mathrm{T,L}} = E^{1+k}\frac{\mathrm{d}N^{\mathrm{T,L}}}{\mathrm{d}E} = \frac{E^k[\mathrm{GeV}]B^{\mathrm{T,L}}(E)[\mathrm{GeV}]}{4\pi d^2[\mathrm{cm}]\hbar[\mathrm{GeV\,s}]}, \tag{22}$$

where d[cm] is the distance to the source, and $4\pi d^2[\mathrm{cm}]\hbar[\mathrm{GeV\,s}] \approx d^2[\mathrm{kpc}]\times 7.877\times 10^{19}$ [17]. It is convenient to rescale $F_E^{\mathrm{T,L}}$ with a power E^k to make steep spectral slopes better visible; we will put $k = 1$. The total differential flux $E^k F_E^{\mathrm{T+L}}[(\mathrm{GeV})^k\,\mathrm{cm}^{-2}\mathrm{s}^{-1}]$ is obtained by adding the polarization components, substituting $B^{\mathrm{T+L}}(E)$ into (22). We find, by assembling (20)–(22),

$$\begin{aligned} E^k F_E^{\mathrm{T+L}} &= \frac{a_{\mathrm{t}}E^{\sigma+k+1}}{(\beta\gamma_{\min})^{\alpha+3}}\Big[(2\alpha(\alpha+1)-(\beta\gamma_{\min})^2)(\beta\gamma_{\min})^{\alpha+1} \\ &\quad\times\Gamma(-\alpha-1,\beta\gamma_{\min})+2\mathrm{e}^{-\beta\gamma_{\min}}(\beta\gamma_{\min}-\alpha)\Big], \end{aligned} \tag{23}$$

with $\gamma_{\min}(E)$ defined in (17). The combined amplitude

$$a_{\mathrm{t}}[(\mathrm{GeV})^k\mathrm{cm}^{-2}\mathrm{s}^{-1}] = \frac{1}{\varepsilon}\frac{\alpha_{\mathrm{t}0}A_{\alpha,\beta}\beta^{\alpha+1}}{4\pi d^2[\mathrm{cm}]\hbar[\mathrm{GeV\,s}]} \tag{24}$$

is a fitting parameter. For a thermal electron population (14) with $\alpha = -2$, the unpolarized flux (23) simplifies to

$$E^k F_E^{\mathrm{T+L}} = \frac{a_{\mathrm{t}}E^{\sigma+k+1}}{(\beta\gamma_{\min})^2}\mathrm{e}^{-\beta\gamma_{\min}}(\beta\gamma_{\min}+2)^2. \tag{25}$$

Weibull decay of the spectral tails of Fermi-LAT pulsars. – We study the high-energy limit $\beta\gamma_{\min}(E) \gg 1$, $\gamma_{\min}(E) \gg 1$, and the intermediate regime $\beta\gamma_{\min}(E) \ll 1$, $\gamma_{\min}(E) \gg 1$, cf. (17), of the unpolarized differential flux density $E^k F_E^{\mathrm{T+L}}$ in (23). The energy range of LAT pulsar spectra [1] lies above 100 MeV. The tachyon-electron mass ratio is assumed to be small, $m_{\mathrm{t}}(E)/m_{\mathrm{e}} \ll 1$, cf. (10), otherwise we would have to quantize the Cherenkov densities (9) (see [18] for the vacuum quantum densities). Thus we can approximate $\gamma_{\min} \sim \kappa_{\mathrm{t}}E^{1-\rho}$ in the LAT spectral range, since $\kappa_{\mathrm{t}}^2 E^{2(1-\rho)} \gg 1$ for $0 \leq \rho < 1$, cf. (17). The above limits correspond to $\beta\kappa_{\mathrm{t}}E^{1-\rho} \gg 1$ and $\beta\kappa_{\mathrm{t}}E^{1-\rho} \ll 1$; the latter is not to be confused with the low-frequency limit $\beta\gamma_{\min}(E\to 0) = \beta$ applicable in the radio band [9], where β and κ_{t} become independent fitting parameters.

In the high-energy regime $\beta\kappa_{\mathrm{t}}E^{1-\rho} \gg 1$, we fit the spectral tail with

$$E^k F_E^{\mathrm{T+L}} \sim A_\infty E^{\eta_\infty}\exp(-\beta_\infty E^{1-\rho}), \quad A_\infty = \frac{a_{\mathrm{t}}}{\beta_\infty^{\alpha+2}}, \tag{26}$$

$$\eta_\infty = \sigma+1+k+(\rho-1)(\alpha+2), \qquad \beta_\infty = \beta\kappa_{\mathrm{t}}. \tag{27}$$

The scaling exponent ρ of the tachyon mass, cf. (10), determines the shape parameter $1-\rho$ of the Weibull exponential in (26), cf. [19].

In the intermediate-energy range (at high temperature), $\beta\gamma_{\min} \sim \beta\kappa_{\mathrm{t}}E^{1-\rho} \ll 1$, the flux reads

$$E^k F_E^{\mathrm{T+L}} \sim \frac{a_{\mathrm{t}}E^{\sigma+k+1}}{(\beta\gamma_{\min})^2}2\Gamma(1-\alpha) = A_0 E^{\eta_0}, \tag{28}$$

$$\eta_0 = \sigma+2\rho+k-1, \qquad A_0 = \frac{a_{\mathrm{t}}}{\beta_\infty^2}2\Gamma(1-\alpha). \tag{29}$$

We restrict here to electron indices $\alpha < 1$ to save notation; this sufficiently covers the equilibrium index $\alpha = -2$. A_0 and η_0 can be estimated by fitting the power-law slope (28) (linear in a log-log plot) to the lower end of the LAT spectrum. The amplitude and scaling relations

$$A_\infty = \frac{A_0}{\beta_\infty^\alpha 2\Gamma(1-\alpha)}, \qquad \eta_\infty = \eta_0+(\rho-1)\alpha \tag{30}$$

are to be substituted into the high-frequency limit (26). We determine initial guesses for A_0 and η_0 from a fit of the ascending slope with (28), insert these parameters into (30), and obtain β_∞, ρ and α by fitting the spectral tail with (26). The fine-structure scaling exponent σ and the flux amplitude a_t are inferred from (29). These parameters serve as initial guess in the χ^2 fit based on (23) or (25), where we substitute $\beta\gamma_\mathrm{min} \sim \beta_\infty E^{1-\rho}$. The fitting parameters are α, σ, ρ, β_∞ and a_t; we will prescribe the electron index, $\alpha = -2$, of an electron gas in thermal equilibrium.

Spectral fits to Fermi-LAT pulsars: sub- and superluminal Cherenkov γ-rays. – In figs. 1–3, we plot the energy flux $EF_E^{\mathrm{T+L}} = E^2\mathrm{d}N^{\mathrm{T+L}}/\mathrm{d}E$, cf. (25), performing tachyonic Cherenkov fits to the LAT spectra of the Vela pulsar, PSR J1709 − 4429 and Geminga. These spectra show distinctly subexponential Weibull decay, $EF_E^{\mathrm{T+L}} \propto \exp(-\beta_\infty E^{1-\rho})$, $\rho > 0$, cf. (26) and table 1. Since the tachyon mass m_t0 is much smaller than the electron mass and the decay exponent $\beta_\infty = \sqrt{\varepsilon\mu_0}\beta/m_\mathrm{t0}[\mathrm{GeV}]$ is moderate, cf. table 1, the temperature parameter β must be small, so that the thermal electron plasma is ultra-relativistic, cf. (14).

The energy dependence of the tachyon mass and the tachyonic fine-structure constant, cf. (10), can be absorbed in the permeabilities, by redefining $\varepsilon(E) = \varepsilon E^{-\sigma}$, $\mu_0(E) = \mu_0 E^{\sigma-2\rho}$ and retaining the relations $\varepsilon(E)\mu(E) = \varepsilon_0(E)\mu_0(E) = 1$, cf. after (9). We can then put $m_\mathrm{t}(E) = m_\mathrm{t0}$, $\alpha_\mathrm{t}(E) = \alpha_\mathrm{t0}$. That is, the spectral functions $B^{\mathrm{T,L}}(E)$ in (20) and (21) do not change if we keep m_t and α_t constant and use frequency-dependent permeabilities instead. The minimal Lorentz factor (17) stays invariant as well, since $\gamma_\mathrm{min}(E) = \sqrt{1+\hat{E}^2}$, $\hat{E} = \sqrt{\varepsilon\mu_0}E/m_\mathrm{t}(E)$.

The refractive indices $n_{\mathrm{T,L}} = k_{\mathrm{T,L}}/\omega$, cf. (7), are related to the transversal and longitudinal group velocities by $\upsilon_{\mathrm{T,L,gr}} = 1/(\omega n_{\mathrm{T,L}})'$. The condition $\varepsilon\mu = \varepsilon_0\mu_0 = 1$ implies $n_\mathrm{T} = n_\mathrm{L}$ and, cf. (10),

$$\upsilon_\mathrm{gr} = \frac{\sqrt{1+E^{2\rho-2}m_\mathrm{t0}^2/(\varepsilon\mu_0)}}{1+\rho E^{2\rho-2}m_\mathrm{t0}^2/(\varepsilon\mu_0)} \approx 1+\left(\frac{1}{2}-\rho\right)E^{2\rho-2}\frac{m_\mathrm{t0}^2}{\varepsilon\mu_0}. \tag{31}$$

Whether this velocity is sub- or superluminal can be read off from the Weibull shape parameter of the spectral tail, cf. (26), from which the scaling exponent ρ of the tachyon mass is inferred: υ_gr is subluminal for $\rho \geq 1/2$ and superluminal for $\rho < 1/2$. Tachyonic γ-rays from the Vela pulsar and PSR J1709 − 4429 are thus subluminal, cf. table 1, whereas the γ-ray emission of Geminga is superluminal. The rescaled tachyonic mass amplitude $m_\mathrm{t0}/\sqrt{\varepsilon\mu_0}$ can be inferred by measuring the group velocity (31); the electron temperature is then obtained via (17), (27) and β_∞ in table 1.

The tachyonic Cherenkov densities (9) are derived from classical Maxwell-Proca equations, cf. (1)–(7), and are independent of the mass of the radiating charge, in contrast to the quantized densities which depend on the tachyon-electron mass ratio; this will be discussed elsewhere.

REFERENCES

[1] Abdo A. A. *et al.*, *Astrophys. J. Suppl. Ser.*, **208** (2013) 17, `http://fermi.gsfc.nasa.gov/ssc/data/access/lat/2nd_PSR_catalog`.
[2] Abdo A. A. *et al.*, *Astrophys. J.*, **713** (2010) 154.
[3] Abdo A. A. *et al.*, *Astrophys. J.*, **720** (2010) 26.
[4] Abdo A. A. *et al.*, *Astrophys. J.*, **708** (2010) 1254.
[5] Abdo A. A. *et al.*, *Astrophys. J.*, **712** (2010) 1209.
[6] Abdo A. A. *et al.*, *Astrophys. J.*, **720** (2010) 272.
[7] Allafort A. *et al.*, *Astrophys. J.*, **777** (2013) L2.
[8] Tomaschitz R., *Phys. Lett. A*, **377** (2013) 945.
[9] Tomaschitz R., *Phys. Lett. A*, **377** (2013) 3247.
[10] Afanasiev G. N., *Vavilov-Cherenkov and Synchrotron Radiation* (Kluwer, Dordrecht) 2004.
[11] Aginian M. A., Ispirian K. A. and Ispiryan M., *EPL*, **104** (2013) 24002.
[12] Treumann R. A., *EPL*, **16** (1991) 121.
[13] Ginzburg V. L., *Phys. Scr.*, **T2A** (1982) 182.
[14] Tomaschitz R., *Phys. Lett. A*, **366** (2007) 289.
[15] Tomaschitz R., *Astropart. Phys.*, **23** (2005) 117.
[16] Tomaschitz R., *Physica A*, **394** (2014) 110.
[17] Nakamura K. *et al.*, *J. Phys. G*, **37** (2010) 075021; `http://pdg.lbl.gov`.
[18] Tomaschitz R., *EPL*, **89** (2010) 39002.
[19] *NIST/SEMATECH e-Handbook of Statistical Methods* (Jan. 2014), `http://www.itl.nist.gov/div898/handbook/eda/section3/eda3668.htm`.